K. Jain C. G. Willson B. J. Lin

Ultrafast High-Resolution Contact Lithography with Excimer Lasers

A new technique for speckle-free, fine-line high-speed lithography using high-power pulsed excimer lasers is described and demonstrated. Use of stimulated Raman shifting is proposed for obtaining the most desirable set of spectral lines for any resist. This permits, for the first time, the optimization of the exposure wavelengths for a given resist, rather than the reverse situation. Excellent-quality images are obtained in 1- μ m-thick diazo-type photoresists such as *AZ-2400 and a diazonaph-thoquinone-*Novolak resist system by means of contact printing with a XeCl laser at 308 nm and a KrF laser at 248 nm. Resolution down to 1000 line pairs per millimeter is experimentally demonstrated. These images are comparable to state-of-the-art contact lithography obtained with conventional lamps. The major difference is that the excimer laser technique is approximately two orders of magnitude faster. Tests on reciprocity failure in several resists indicate a decrease in sensitivity by only a factor of three, despite the $\approx 10^8$ times larger power density used in the laser exposures. The possibility of photochemical reactions being different from those taking place in the case of lamp exposures is discussed in view of these results.

Introduction

In optical lithography, the improvement in resolution resulting from the use of shorter wavelengths is well known. The dependence of the resolution w on the wavelength λ is given by $w \approx \lambda/2NA$ for projection printing and by $w^2 \approx \lambda z/2$ for proximity printing, where NA is the numerical aperture of the imaging lens and z is the mask-to-wafer gap. In projection printing, w improves in proportion to the decrease in λ . However, this is accompanied by a proportional reduction in the depth of the field, which is given by $Z \approx \lambda/NA^2$. Nevertheless, use of shorter wavelengths as a means to improve resolution is more desirable than increasing NA because the loss in depth of field is faster in the latter case. In proximity or contact printing, the minimum feature size decreases as $\sqrt{\lambda}$. Alternatively, to preserve the same feature size, z can be increased in proportion to the reduction in λ .

These considerations have motivated a large amount of research effort in deep-ultraviolet (200–300-nm) lithography [1]. The light source traditionally used in all deep-uv systems to date has been either a deuterium (D_2) lamp or an Xe-Hg arc lamp. The problem with using such lamps is that not enough power is available in the desired spectral region.

For example, the total deep-uv power that can be collected from a 1-kW Xe-Hg lamp, using 0.07-NA optics, is ≈16 mW [2]. Simply making the lamps bigger is not as trivial as it appears because of problems associated with removal of the heat generated by the unwanted radiation. Consequently, the exposure times required for resists sensitive in the deep uv, such as poly(methyl methacrylate) (PMMA), are typically several minutes [2]. In contrast, with the use of excimer lasers with deep-uv power outputs of >10 W, a 12-13-cm wafer can be exposed in a few seconds-an improvement by ≈2 orders of magnitude. It should be pointed out that previous attempts at photolithography with laser light sources have been limited to the use of continuous-wave (cw) sources in the visible, and to exposure systems using either scanning-spot techniques [3, 4] or nonlinear optical effects [5], both of which to date have required very long exposure times. Another direction that lithographic research has taken involves development of suitable resists with optimum spectral characteristics to match emission lines available from various conventional lamps. With the stimulated-Raman-shifted excimer laser approach described

Copyright 1982 by International Business Machines Corporation. Copying is permitted without payment of royalty provided that (1) each reproduction is done without alteration and (2) the *Journal* reference and IBM copyright notice are included on the first page. The title and abstract may be used without further permission in computer-based and other information-service systems. Permission to republish other excerpts should be obtained from the Editor.

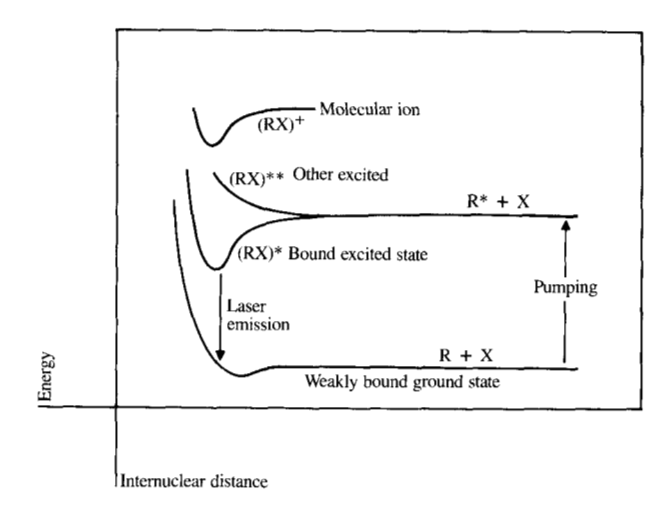


Figure 1 Typical potential energy curves for rare-gas monohalide molecules showing a laser transition from a bound upper level to an unstable ground state.

here, this problem is considerably eased. By properly choosing the Raman medium and by optimizing various parameters, such a system can produce one or several wavelengths anywhere in a wide spectral region. Therefore, for the first time, the exposure wavelength can be optimized for the given resist, rather than the reverse.

The extremely short exposure times obtainable by excimer-laser lithography have another important consequence. When the exposure time becomes a negligible part of the entire device fabrication cycle, the *photosensitivity of the resist is no longer an issue* in determining the wafer throughput. Thus, the choice of the resist can be optimized on the basis of its other properties, such as image resolution and aspect ratio, adhesion, wet-etch characteristics, reactive ion etch rate, coating properties, and stability. This advantage would be significant in providing processing flexibility and potentially larger process windows.

The source

Excimer lasers

Excimer lasers are a new class of very efficient and powerful pulsed uv lasers [6] that became commercially available in 1978. They emit several characteristic wavelengths from below 200 nm to above 400 nm, depending on the laser medium. For example, the following lasing media give transitions at the wavelengths (nm) indicated: ArF, 193; KrCl, 222; KrF, 249; XeBr, 282; XeCl, 308; and XeF, 351. In addition, several excimer lasers have been demonstrated in the vacuum-uv region. Overall energy conversion efficiencies of >1% and average output powers of several tens of watts in the deep uv have already been reported [6]. Several excitation schemes have been successfully demonstrated in

the laboratory, and simple high-power discharge-pumped systems are now commercially available.

Prior to the advent of excimer lasers, uv lasers operating below 300 nm had been limited to multiply ionized noble-gas lasers [7, 8] and singly ionized metal-vapor lasers [9, 10]. The multiply ionized noble-gas lasers require threshold current densities of ≈10³ A/cm² and have poor efficiencies (<0.01%). The metal-ion lasers can be made physically small and run in cw mode, but the best overall efficiencies achieved to date (<0.002%) are even worse than those for the noble-gas lasers. In addition, neither of these types of lasers has been able to produce average output powers greater than a few milliwatts in the deep uv and neither has been made commercially. Other means of generating coherent deep-uv radiation have utilized nonlinear techniques such as harmonic generation and frequency mixing [11], but such systems also require very large pump powers and have poor efficiencies, rendering them unattractive. The excimer lasers overcome many of these shortcomings. They can have extremely high efficiencies, can achieve very high average power output, and can be made very compact. Their major drawback seems to be the short life ($\approx 10^{6}$ shots) of a gas fill; however, recent work points to the possibility of significant improvement in this area.

Excitation mechanism

The large family of molecules known as excimers are characterized by a bound excited state and an unstable or very weakly bound ground state. We concern ourselves with a subset of excimer lasers known as rare-gas halide (RGH) lasers. The latter lase on transitions of molecules of the type RX, where R and X denote a rare-gas atom and a halogen atom, respectively. Typical potential energy curves for an RGH molecule are shown in Fig. 1. Population inversion is readily produced because the lower-level dissociation time $(\approx 10^{-12} \text{ s})$ is much less than the upper-level radiative lifetime (10⁻⁹-10⁻⁶ s). Excitation to the upper state RX* can be produced by several mechanisms. Since the excited state is the same as the ion pair R⁺X⁻, recombination of the positive rare-gas ions and the negative halogen ions populates the upper level. The positive and negative ions are readily produced by high-energy electron collisions. Still another way of producing the upper laser state involves reaction between R* and a halogen compound; for example,

$$Xe^* + NF_3 \rightarrow (XeF)^* + NF_2$$
.

Several different approaches have been used to pump excimer lasers. Four of the most commonly used are 1) direct excitation by a high-energy electron beam, 2) excitation by an electric discharge that is controlled by an electron beam, 3) direct electric-discharge excitation, and 4) optical pumping. Of these, the direct electric discharge is the most practical in terms of compactness and ease of operation. Typically, efficient excitation by discharge pumping re-

quires a spatially uniform, high-voltage discharge in gas mixtures at pressures of several hundreds of kilopascals (several atmospheres) with discharge gaps of a few centimeters. This is most successfully done with a transverse discharge, using some sort of pre-ionization of the gas mixture prior to the main discharge pulse. This transversely excited atmospheric (TEA) pressure discharge geometry has been widely used for high-power CO_2 lasers, and excimer lasers using the same basic design are now commercially available.

Power output

Commercially available excimer lasers now readily provide several watts of average power at a number of wavelengths. For example, a Lumonics Model TE-861 laser, which was optimized for operation with KrF, provides the following approximate average power levels (W) at the indicated representative excimer laser lines: ArF, 10; KrCl, 2; KrF, 20; XeCl, 8; and XeF, 7. In laboratory versions, average power outputs up to 200 W have been reported [12]. A commercial unit that uses wide-gap electrodes (Lumonics Model TE-290) can provide single-pulse energies up to 1.5 J.

Pulse width and repetition rate

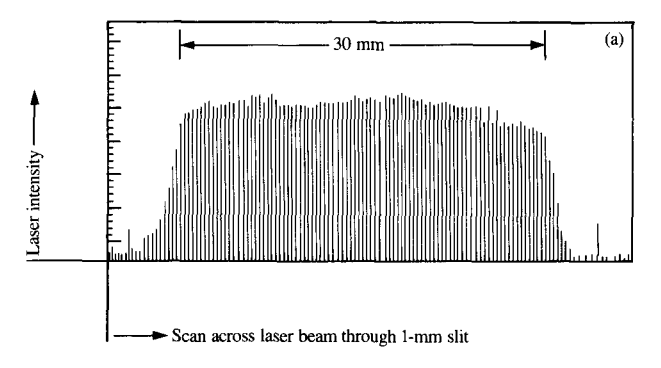
With discharge-pumped systems the obtainable pulse widths are typically $\approx 10-100$ ns. Thus, the peak powers are $\approx 10^7$ W. For longer pulses, electron-beam-pumped systems are more convenient. For systems with average power in the several-watt range, the available repetition rates vary from single pulses to ≈ 1 kHz. However, for currently available lasers with pulse energies >1 J, the repetition rates are limited to ≈ 1 Hz because of the accumulation of photoproducts that absorb in the uv. Advances in this direction are possible with the use of gas-handling systems capable of faster flow rates.

Beam uniformity and mode structure

The beam cross section depends on the electrode geometry, and thus, can be optimized over a wide range, depending on the application. Lumonics Models TE-861 and TE-290 have rectangular beam shapes of 7×20 mm and 25×30 mm, respectively. The uniformity of the intensity across a major portion of the beam is excellent [see example in Fig. 2(a)]; it arises because the mode structure of these transversely excited beams is extremely non-Gaussian. In fact, it is so highly multi-mode and random that interference effects due to spatial coherence in a transverse plane are nonexistent in our lithography experiments.

Power stability

In most excimer laser systems, the output power rapidly decays with time because of degradation of the gas mixture caused by its corrosive nature and formation of photoproducts that absorb at the laser wavelength. Improvements have been made by recirculating and cooling the gas mixture



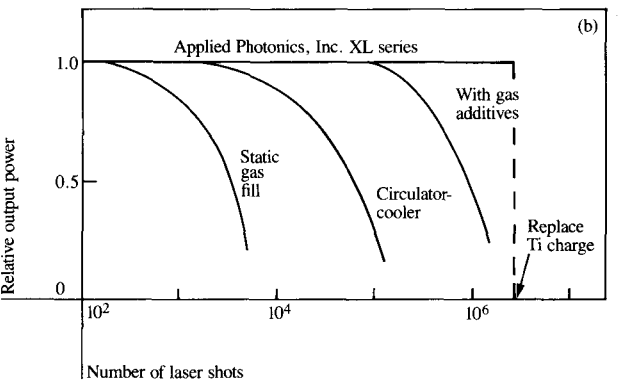


Figure 2 (a) Intensity uniformity across the beam of the Lumonics Model TE-290 KrF laser. (b) Stability of the output power as a function of the number of shots for various excimer laser systems. The dashed line indicates saturation of the Ti charge in the purifier ovens; revival of laser performance to full power is readily achieved by replacement of the charge.

and by introducing small amounts of additives such as hydrogen into the discharge. With a multi-stage purifier-recirculator system (Applied Photonics, Inc., XL series), constant output power has been reported for $>2 \times 10^6$ pulses with a KrF laser. At a repetition rate of 100 Hz, this gives ≈ 6 h of operation with no degradation in power [Fig. 2(b)]. For the XeCl laser at 308 nm, the performance is even better.

• Stimulated Raman shifting

Spontaneous Raman scattering is the process by which the radiation incident on a material experiences a frequency shift due to inelastic scattering from certain characteristic excitations (e.g., molecular vibrations) of the medium. When the incident power is made large enough, this frequency-shifted scattered radiation can be stimulated. Whereas the conversion yield in the spontaneous Raman effect is typically $\approx 10^{-7}$, it can be as large as 0.7 in the stimulated case. Thus, intense coherent light can be produced at different wavelengths by stimulated Raman scattering. The scattered wavelengths can be both up(Stokes)- and down(anti-Stokes)-shifted from the incident laser wavelength by multiples of a molecular vibration (or other elementary excitation) characteristic of the Raman medium.

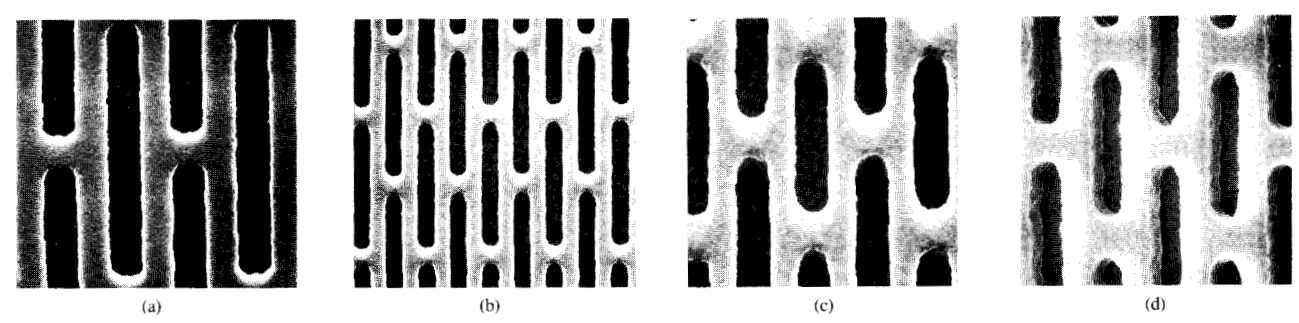


Figure 3 SEMs of images obtained in AZ-2400 photoresist with a XeCl laser at 308 nm: dimensions of lines and spaces are (a) 2 μ m, (b) 1 μ m, and (c) 0.5 μ m. (d) An oblique view of (c) showing a trace of standing waves. The exposures were made with two 10-ns-wide, 50-mJ/cm² laser pulses.

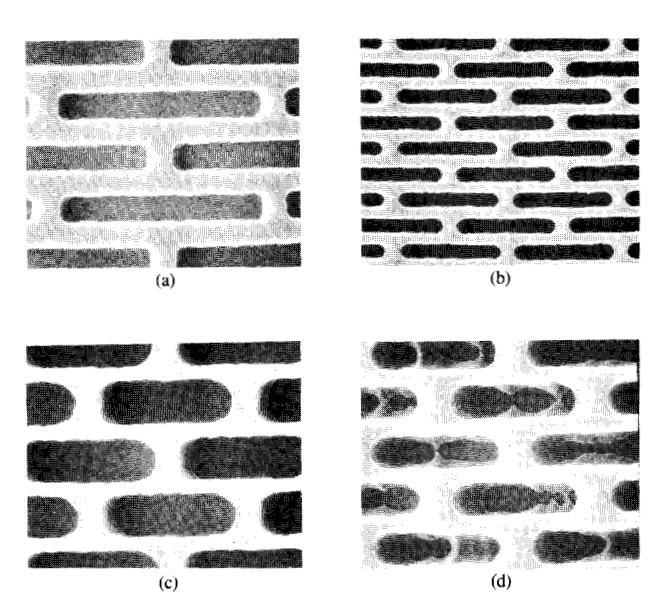


Figure 4 Images obtained in DNN photoresist with one 50-mJ/cm² XeCl pulse: (a) 2- μ m lines and spaces, (b) 1- μ m lines and spaces, (c) 667 line pairs/mm, overdeveloped, and (d) 1000 line pairs/mm, underdeveloped.

Since very high peak powers are available from excimer lasers, they are ideally suited for stimulated Raman shifting. Thus, each of the wavelengths produced by the excimer lasers can be shifted to several new wavelengths by selecting different Raman media. As an example, we cite the work of Loree et al. [13], who have obtained many different sets of Stokes- and anti-Stokes-shifted lines spanning the range from 190 to 415 nm by stimulated Raman scattering in H₂, D₂, CH₄, and liquid N₂, using ArF, KrF, KrCl, and XeCl lasers. Moreover, as the same authors point out, the distribution of the incident laser pulse energy into various modes can be tailored by adjusting the gas pressure and/or the optics.

Thus, for any photoresist the most desirable wavelength(s) can be produced by properly selecting the excimer

laser and the Raman-shifting conditions. We point out that good mode quality is required from the laser for efficiently pumping a Raman cell. Optics for diffraction-limited resonators necessary for such mode quality are now available with commercial excimer lasers. However, the absence of speckle in imaging with a Raman beam remains to be demonstrated.

Contact lithography with excimer lasers

Two excimer lasers, KrF (249 nm) and XeCl (308 nm), were used for our lithographic experiments. The KrF laser was a Lumonics Model TE-290 and the XeCl was a Lumonics Model TE-861. All exposures were made with the raw unprocessed beams from the lasers. Three resists were investigated for image quality and photosensitivity characterization: *AZ-2400, a diazonaphthoquinone-*Novolak (DNN) resist, and an oxodiazonaphthalene-sulfomethyl-tricyclodecane (OST) resist.

Imaging experiments

Our imaging exposures were made by contact printing using a brick-pattern mask with feature sizes varying from 0.5 to $2.0 \mu m$, in $0.25 - \mu m$ steps. The chromium mask on a quartz substrate was held in contact with a 2.5-cm-diameter Si wafer by vacuum. The wafer was coated with a 1-μm layer of resist. The XeCl laser beam incident on the wafer had a cross-sectional area of ≈1 cm² and an energy of ≈50 mJ/ pulse. The pulses were ≈10 ns wide, giving a peak power density of 5 MW/cm². The images in the AZ-2400 photoresist for feature sizes of 0.5, 1, and 2 μm, shown in scanning electron micrographs (SEMs) in Figs. 3(a)-(d), were made with two laser pulses. Thus, the total dose was ≈100 mJ/ cm², delivered in ≈20 ns. After exposure, the wafers were developed for 2 min in a solution consisting of 1:4 *AZ-2401 developer/water. Note the excellent image quality and total absence of speckle. The latter result, as mentioned previously, is due to the highly random mode structure of the laser output. This randomness produces an exposure as if it had been made by several independent multi-mode lasers. The

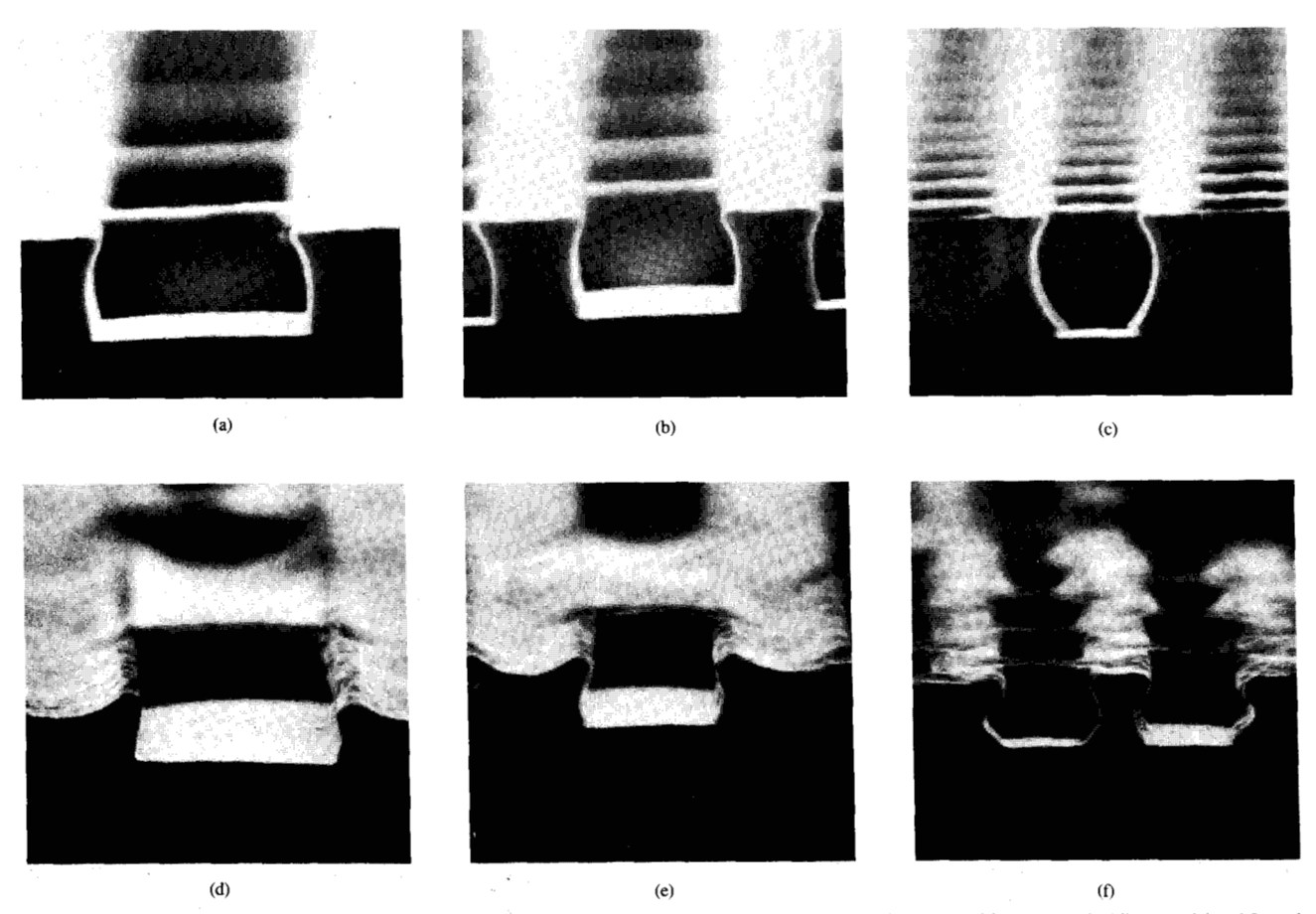


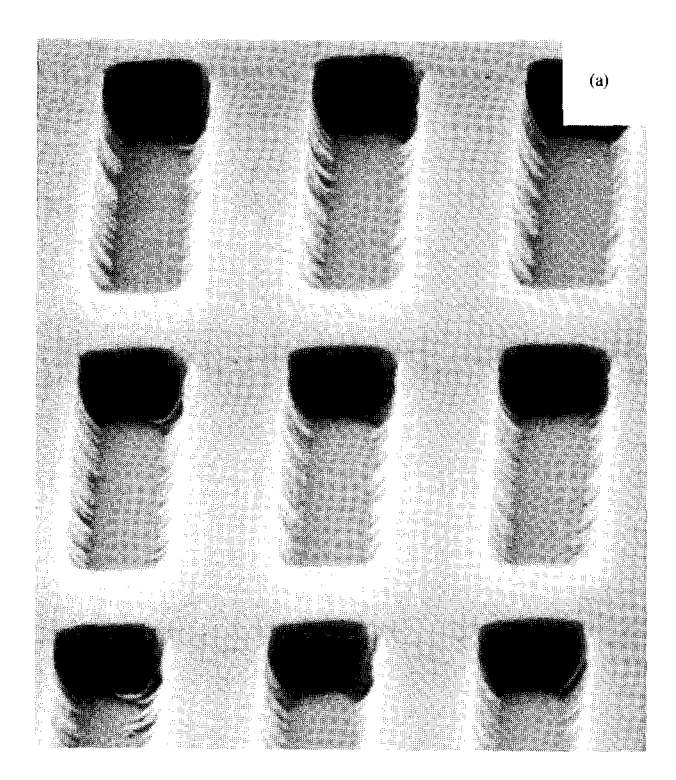
Figure 5 Sidewall profiles of features of various sizes (in μ m) in DNN: (a) 1.75, (b) 1.25, and (c) 0.5; and in AZ-2400: (d) 1.75, (e) 1.25, and (f) 0.5. The exposures were the same as in Figs. 3 and 4.

resulting lack of spatial coherence in a transverse plane serves to wash out speckle in our experiments. The large bandwidth (≈ 1.5 nm), and hence the poor temporal coherence of the laser emission, also contributes to the reduction of speckle. The absence of speckle was also confirmed by a large-area pad exposure, in which no structure due to speckle was seen on development.

With a monochromatic light source, one also expects to see standing waves due to interference between incident radiation and that reflected from the substrate or from the resist-air interface. Figure 1(d) shows that standing-wave effects in this exposure, though not totally absent, are barely noticeable. Thus, the standing-wave problem here is surprisingly close to negligible, perhaps because cancellation of light intensity at the interference nodes is not perfect and because the resist receives significant exposure even at these points. It is also possible that resist heating contributes to the reduction in standing-wave effects [14].

Images obtained with the same mask in 1 μ m of DNN are shown in Figs. 4(a)–(d). Here, the wafer was irradiated with one laser pulse for a dose of ≈ 50 mJ/cm² and developed for 3 min in a 1:3.5 solution of AZ-2401/water. The 1- and 2- μ m images are as good or better than those obtained in AZ-2400. The 0.75- μ m images, although of excellent quality, appear to be overdeveloped. On the other hand, the 0.5- μ m lines are underdeveloped. Thus, our development procedure is not optimum for the smaller features made in this resist.

Sidewall profiles of the 1.75, 1.25, and 0.5-µm features in AZ-2400 and DNN are shown in Figs. 5(a)-(f). The exposures were the same as those used to obtain the images of Figs. 3 and 4. Note the excellent wall definition and undercut. The latter results from a combination of the free-space images with vertical walls, characteristic of contact printing, and the induction phenomenon in the resist, which is known to occur in both resists and which gives a faster dissolution rate with increasing development depth.



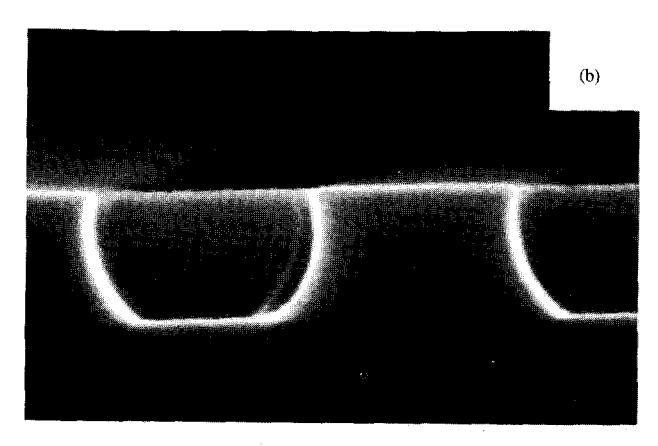


Figure 6 (a) 1.5-µm lines and spaces in AZ-2400 obtained with a KrF laser at 248 nm. The exposure dose was 125 mJ/cm². (b) Cross section of (a) showing wall profile.

Figure 6 shows 1.5- μ m lines and spaces obtained in AZ-2400 using the KrF laser at 248 nm. The total dose of 125 mJ/cm² was delivered in five pulses with an attenuated laser output of 25 mJ/cm² per pulse. The wafer was developed for 30 s in a 1:4 solution of AZ-2401 developer and water. Note again the absence of speckle and the expected wall profile.

Photosensitivity characterization

A quantitative determination of resist sensitivity with laser exposure is important because with the large power densities involved, one may expect to see effects such as loss of

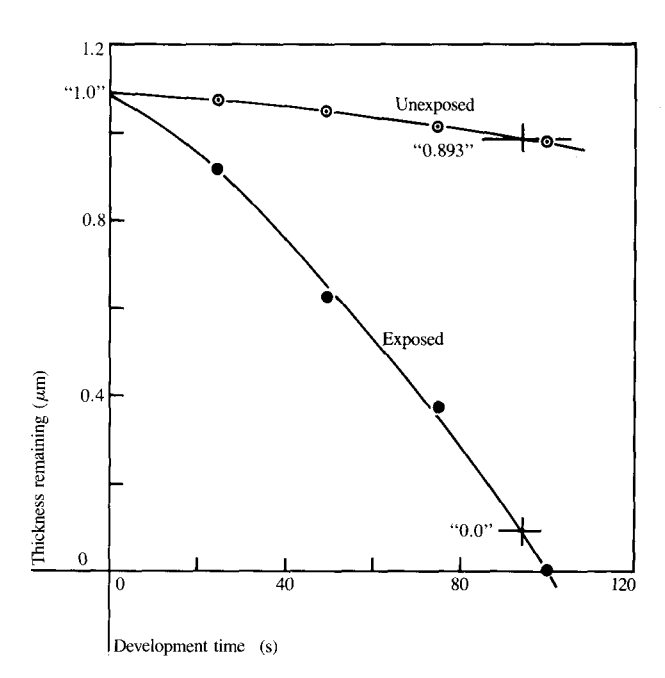


Figure 7 Method illustrating the definition of photoresist sensitivity. The exposed and unexposed thicknesses are measured as a function of the development time for various exposure doses.

reciprocity. Several ways of describing the sensitivity of a photoresist have been reported [1, 15, 16]. For the purpose of this study, the sensitivity will be defined as follows. Several 1- μ m-thick films of the resist material are exposed with various doses of the incident radiation. The wafers are developed until the exposed region in each case is completely removed. The remaining thickness of unexposed region is then measured. A plot is made of this thickness νs , the dose. The intensity at which the linear portion of this curve extrapolates to a remaining thickness of 1 μ m is defined as D_s , the photosensitivity of the resist. It is evident that D_s alone does not completely describe the resist performance; thus, one must also consider the slope of the curve and the time required to develop to the end point at a specific dose.

Figure 7 illustrates the method. A nominally 1- μ m-thick film of DNN was given a pad exposure of 24 mJ/cm² in four different regions of a 5-cm-diameter wafer. The four regions were developed for different times and the remaining thicknesses of the exposed and unexposed regions were plotted in the figure. The "0.0" film thickness was defined as 1.0 μ m less than the actual original thickness (1.09 μ m). The "normalized" remaining thickness of the unexposed resist was found to be 0.893 μ m. Similar measurements were made at incident intensities of 50, 100, and 150 mJ/cm². The variations of the thicknesses remaining ν s. the doses for AZ-2400, DNN, and OST are shown in Fig. 8. From the intercept at a thickness of 1.0 μ m, the sensitivity for all

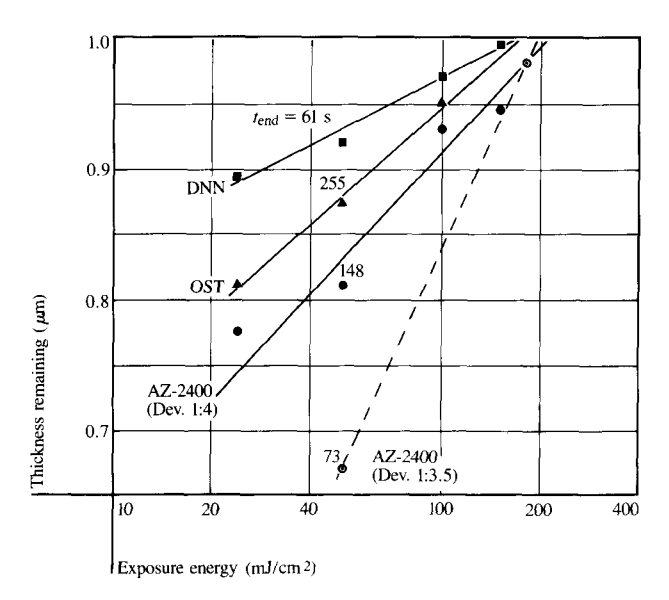


Figure 8 Photosensitivity of various resists with XeCl laser irradiation obtained by plotting the remaining thickness of unexposed resist vs. the dose. The end-point development times with a 50-mJ exposure are also shown.

resists is seen to be $\approx 200 \text{ mJ/cm}^2$. To determine the extent of reciprocity failure, the sensitivity of the resists was also measured at conventional power levels (a few mW/cm²). Results for AZ-2400 exposed with the 313-nm line from a Xe-Hg lamp gave a D_s of 70 mJ/cm². Thus, there is a loss in sensitivity by approximately a factor of three with laser irradiation for AZ-2400. This is surprising, considering the $\approx 10^8 \times$ increase in the power density using the excimer laser. Thus, it can be concluded that reciprocity failure is not a significant problem in pulsed excimer laser lithography.

Figure 9 shows the dissolution rates of exposed and unexposed resist as functions of the exposure energy. Note that both the abscissa and ordinate are logarithmic. In addition to the general nonlinearity of the curves, the behavior at low exposure energies indicates saturation since the slopes are «1. However, the slopes at higher exposures rise rapidly, and it will be interesting to determine whether this is due to the onset of multi-photon processes in the resist.

• Discussion

The quality of images obtained with the laser exposures is comparable to state-of-the-art lithography using Hg lamps. This is encouraging and points to the possibility that excimer-laser lithography may be a promising lithographic technique. We have already mentioned its advantage in terms of higher speed. Stimulated Raman shifting makes it possible to have this high speed at any wavelength by

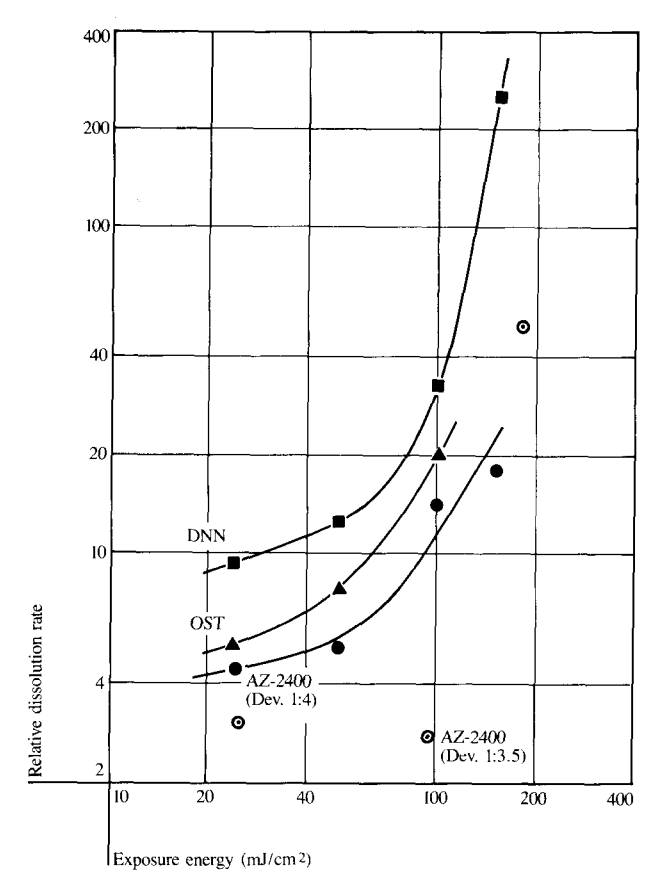


Figure 9 The relative dissolution rate as a function of the exposure energy for various resists.

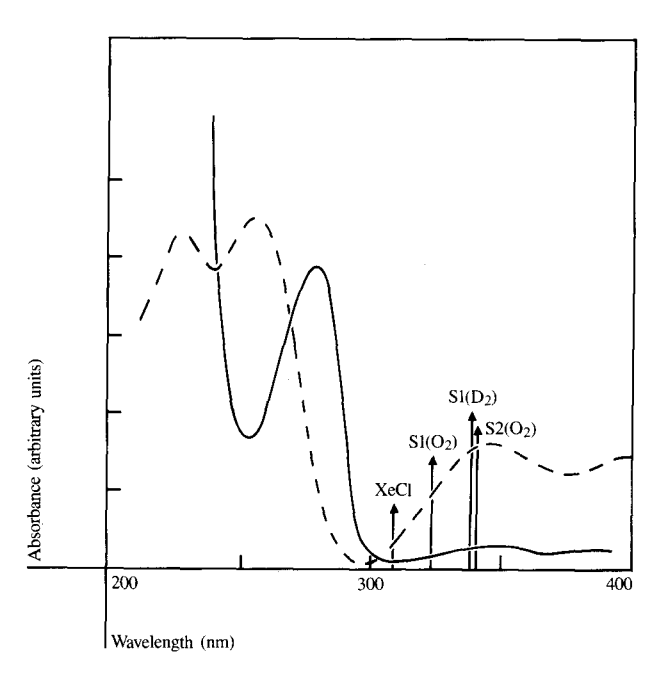


Figure 10 Absorbance spectra of diazonaphthoquinone sensitizer and ${}^{\circ}$ Novolak resin, along with the first- and second-Stokes Raman lines from O_2 , and the first-Stokes line from O_2 with a XeCl laser.

bringing the laser energy near the peak of the resist performance curve. An example is shown in Fig. 10, where the absorbance spectra of diazonapthoquinone sensitizer and ®Novolak resin and several Stokes-shifted Raman lines obtained using the XeCl laser are superimposed.

From the point of view of collimation, since the laser is a far better light source than a Hg or D, lamp, design of the optics in a deep-uv contact printer should be considerably simpler. The availability of suitable optical materials in the deep uv is not a problem, since they are already being used with current lamp systems. Speckle, thought to be the most formidable problem with laser lithography, has been demonstrated to be absent. Image degradation due to standing waves, although not totally absent, is found to be minimal, and it can be further reduced by the use of multi-wavelength exposure, which is possible with a Raman shifter. In addition, coherence effects can be reduced by several techniques previously used in conventional lithography; e.g., use of oblique phase fronts obtained by one or more rotating mirrors [1, 17, 18], use of a "fly's eye" lens optical integrator [19], moving the wafer, or use of a random phaseretardation plate.

The major difference between conventional-lamp-lithography and excimer-laser images is that in the latter the relative power density is eight orders of magnitude greater. One might thus expect severe reciprocity failure in the laser exposures. Previously, using a two-step kinetic model applicable to both positive and negative photoresists, Albers and Novotny [20] calculated the intensity dependence of photochemical reaction rates and found that saturation would occur for intensities $\gtrsim 5 \text{ kW/cm}^2$. In view of the fact that our laser exposures were made with intensities of $\approx 10 \text{ MW/cm}^2$, the loss in sensitivity only by a factor of three is indeed surprising. In our view, it is unlikely that the photochemical processes taking place in the two cases are the same. Turro et al. [21] have observed that the photoproducts produced by KrF-laser-excited diphenyldiazomethane and tetraphenyloxirane are different from those produced by conventional-lamp excitation of the same substances. It is also improbable that the effect of the intense laser pulse is purely thermal because large thermal diffusion lengths in the resist (a dielectric) would preclude good image definition. We believe that multi-photon effects are at least partially responsible for the behavior of photoresists under excimerlaser exposure, and it may be interesting to investigate this further from an organic photochemical viewpoint.

Summary

A new technique for fast high-resolution photolithography with uv excimer lasers has been proposed and demonstrated. Excellent-quality speckle-free high-resolution images were obtained in the AZ-2400 and diazonaphthoquinone-®Novo-

lak photoresists with XeCl and KrF lasers. Studies were presented of reciprocity failure in several resists in going from exposure with a Hg lamp to the excimer laser, and a loss in sensitivity by only a factor of three was found. A brief review of excimer lasers and the technique of stimulated Raman shifting was given, and use of the latter in obtaining the most suitable wavelength(s) for any resist was discussed. It was pointed out that the exposure times needed with excimer lasers can be so short that the photosensitivity need not be a major factor in selecting an optimum resist; i.e., the resist can be selected on the basis of its other desirable characteristics.

Acknowledgments

The authors are indebted to P. P. Sorokin and D. S. Bethune for loan of their equipment and for assistance with the experiments. They also thank V. E. Hanchett for taking SEM photographs and M. D. Levenson for his stimulating discussions.

References and notes

- See for example B. J. Lin, "Optical Methods for Fine Line Lithography," Fine Line Lithography, Roger Newman, Ed., North-Holland Publishing Co., New York, 1980, pp. 105-232.
- Burn Jeng Lin, "Deep UV Lithography," J. Vac. Sci. Technol. 12, 1317-1320 (1975).
- 3. R. A. Becker, B. L. Sopori, and W. S. C. Chang, "Focused Laser Lithographic System," Appl. Opt. 17, 1069-1071 (1978).
- M. Lacombat, G. M. Dubroeucq, J. Massin, and M. Brevignon, "Laser Projection Printing," Solid State Technol. 23, No. 8, 115-121 (1980).
- 5. M. D. Levenson, "High Resolution Imaging by Wave-Front Conjugation," Opt. Lett. 5, 182-184 (1980).
- For an excellent review, see James J. Ewing, "Rare-Gas Halide Lasers," Phys. Today 31, 32-39 (May 1978).
- 7. Gail A. Massey, Brian P. Plummer, and Joel C. Johnson, "A High Repetition Rate Ion Laser Spanning the 195-225 nm Spectral Region," *IEEE J. Quantum Electron.* **QE-14**, 673-679 (1978).
- 8. John B. Marling, "Ultraviolet Ion Laser Performance and Spectroscopy—Part I: New Strong Noble-Gas Transitions Below 2500 Å," *IEEE J. Quantum Electron.* **QE-11,** 822–834 (1975).
- J. R. McNeil, R. D. Reid, D. C. Gerstenberger, and G. J. Collins, "Ultra-violet Ion Lasers," High-Power Lasers and Applications, K. L. Kompa and H. Walther, Eds., Springer-Verlag, New York, 1978, pp. 89-91.
- Kanti Jain, "A Milliwatt-Level CW Laser Source at 224 nm," Appl. Phys. Lett. 36, 10-11 (1980).
- Michael D. Jones and Gail A. Massey, "Milliwatt-Level 213 nm Source Based on a Repetitively Q-Switched, CW-Pumped Nd:YAG Laser," *IEEE J. Quantum Electron.* QE-15, 204–206 (1979).
- 12. T. S. Fahlen, "200 W KrF Gas Transport Laser," *IEEE J. Quantum Electron.* **QE-16**, 1260-1262 (1980).
- T. R. Loree, R. C. Sze, D. L. Barker, and P. B. Scott, "New Lines in the UV: SRS of Excimer Laser Wavelengths," *IEEE J. Quantum Electron.* QE-15, 337-342 (1979).
- Edward John Walker, "Reduction of Photoresist Standing-Wave Effects by Post-Exposure Bake," *IEEE Trans. Electron Devices* ED-22, 464-466 (1975).
- 15. Dietrich Meyerhofer, "Photosolubility of Diazoquinone Resists," *IEEE Trans. Electron Devices* **ED-27**, 921-926 (1980).
- M. C. King, "Emerging Technology of 1:1 Optical Projection Lithography," Digest of Papers, pp. 294–297, IEEE Computer

- Soc. 20th International Conference, COMPCON, San Francisco, CA, Feb. 25–28, 1980; IEEE Catalog No. 80CH1491-OC.
- J. K. Houston, "Lithography," U.S. Patent No. 3,795,446, 1974.
- 18. B. J. Lin, "Optical Manipulation of Resist Profiles in Conformable Printing," J. Vac. Sci. Technol. 15, 1012-1015 (1978).
- 19. Used in the Canon 500 system.
- John Albers and Donald B. Novotny, "Intensity Dependence of Photochemical Reaction Rates for Photoresists," J. Electrochem. Soc. 127, 1400-1403 (1980).
- 21. Nicholas J. Turro, Masayuki Aikawa, Jared A. Butcher, Jr., and Gary W. Griffin, "Organic Photochemistry: The Laser vs.

the Lamp. The Behavior of Diphenylcarbene Generated at High Light Intensities," J. Amer. Chem. Soc. 102, 5127-5128 (1980).

Received April 9, 1981; revised October 7, 1981

K. Jain and C. G. Willson are located at the IBM Research Division laboratory, 5600 Cottle Road, San Jose, California 95193. B. J. Lin is located at the IBM Thomas J. Watson Research Center, P.O. Box 218, Yorktown Heights, New York 10598.